PHILOSOPHICAL TRANSACTIONS OF THE ROYAL SOCIETY A MATHEMATICAL, PHYSICAL & ENGINEERING SCIENCES

The Geochemical and Tectonic Evolution of the Central Karakoram, North Pakistan [and Discussion]

A. J. Rex, M. P. Searle, R. Tirrul, M. B. Crawford, D. J. Prior, D. C. Rex, A. Barnicoat and J.-M. Bertrand

Phil. Trans. R. Soc. Lond. A 1988 **326**, 229-255
doi: 10.1098/rsta.1988.0086

Phil. Trans. R. Soc. Lond. A **326**, 229–255 (1988) [229]
Printed in Great Britain

The geochemical and tectonic evolution of the central Karakoram, North Pakistan

By A. J. Rex,[1] M. P. Searle,[1] (the late) R. Tirrul,[2] M. B. Crawford,[1] D. J. Prior,[3] D. C. Rex,[3] and A. Barnicoat[4]

[1] *Department of Geology, University of Leicester, Leicester LE1 7RH, U.K.*
[2] *Geological Survey of Canada, 588 Booth Street, Ottawa, Ontario, Canada K1A 0E4*
[3] *Department of Earth Sciences, University of Leeds, Leeds LS2 9JT, U.K.*
[4] *Department of Geology, University College of Wales, Aberystwyth, Dyfed SY23 3DB U.K.*

The Main Karakoram Thrust (MKT) separates the Karakoram Plate from the accreted Kohistan–Ladakh Terranes and Indian Plate to the south. Within the central Karakoram three geologically distinct zones are recognized: from south to north (i) the Karakoram metamorphic complex, (ii) the Karakoram batholith and (iii) the northern Karakoram sedimentary terrane.

Magmatic episodes of Jurassic and mid-Upper Cretaceous age are recognized before India–Asia collision at *ca.* 50–45 Ma. Both reveal subduction-related petrographic and geochemical signatures typical of Andean-type settings. Associated with the Jurassic event was a low-pressure metamorphism (M1). Synchronous with the mid-Upper Cretaceous episode was the passive accretion of the Kohistan–Ladakh terrane to the Karakoram and closure of the Shyok Suture Zone (SSZ). The main collision between the Indian and Asian Plates resulted in crustal thickening beneath the Karakoram and development of Barrovian metamorphism (M2). Early post-collisional plutons dated at 36–34 Ma cross-cut regional syn-metamorphic foliations and constrain a maximum age on peak M2 conditions. Uplift of the Karakoram metamorphic complex in response to continued crustal thickening was synchronous with culmination collapse along the inferred Karakoram Batholith Lineament (KBL). A combination of thermal re-equilibration of thickened continental crust and the proposed addition of an enriched mantle component promoted dehydration, partial melting and generation of the Baltoro Plutonic Unit (BPU). It was subsequently emplaced as a hot, dry magma into an extensional mid-crustal environment. A contact aureole (M3) was imposed on the low-grade sediments along the northern margin, whereas isograds in uplifted metamorphic rocks to the south were thermally domed with *in situ* migmatization.

Introduction

The inter-relations of crustal melting and metamorphic processes within continent–continent collision zones have been widely addressed (England & Thompson 1984, 1986). Thickening of continental crust comprises two end-member geometries: underthrusting of one crustal sheet beneath another (single thrust model) and homogeneous thickening of the entire lithosphere. Thermal relaxation and regional metamorphism then occur synchronous to thinning of the crust by erosion. More rapid exhumation may also occur through differential uplift of fault-bounded blocks. The pressure–temperature–time (P–T–t) paths followed by rocks in this environment (England & Thompson 1984) suggests that considerable melting of the crust is inevitable, the amount dependent upon water availability. Where there is a delay of some

20–30 Ma between crustal thickening and the onset of extension, large volumes of melt are expected (England & Thompson 1986). The High Himalayan granites, products of thermal re-equilibration after India–Asia collision, were water-saturated melts that migrated short distances through the crust. However, crustal melting under water-saturated conditions is generally considered to be the exception, the rule being that crustal melting occurs under fluid-absent conditions (see Clemens & Vielzeuf 1987).

In this contribution we document the metamorphic and magmatic history of the Karakoram Range, north Pakistan. The well-constrained tectonic framework allows both pre- and post-collisional processes to be studied. The magmatic history is emphasized, especially the tectonic implications that arise through interpretation of geochemical and isotopic data (Pearce *et al.* 1984; Harris *et al.* 1986). It is shown that geochemical constraints, when integrated with other evidence, provide important insights into the development of the Karakoram.

Tectonic framework

The mountain ranges of the Karakoram extend from the Afghanistan–Pakistan border eastwards, along the northern frontiers of Pakistan and India with the Chinese province of Xinjiang, to western Tibet. Two regions of the central Karakoram have been studied in detail and represent the basis to the tectonic interpretations presented here. The first region is the Hunza Valley and satellite valleys and the second is the Baltoro–Shigar–Hushe area (figure 1).

Early reconnaissance studies of the Hunza region were made by Desio & Martina (1972) with more recent studies of specific geological zones including Le Fort *et al.* (1983), Prior (1987) and Debon *et al.* (1987). Early reconnaissance work in the Baltoro glacier region includes Lydekker (1883), Auden (1935, 1938) and Schneider (1957). Geological maps were published on the basis of the Italian expeditions to the Karakoram and Hindu Kush in 1953 and 1954 (Zanettin 1964; Desio & Zanettin 1970). The Hushe valley was described by Desio & Mancini (1974) and the Biafo–Hispar area by Desio *et al.* (1985). Recent studies in the Baltoro and Hushe regions include Bertrand & Debon (1986), Debon *et al.* (1986*a*), Brookfield (1980, 1981), Brookfield & Reynolds (1981), Reynolds *et al.* (1983) and Searle *et al.* (1988). A more regional synthesis on the evolution of the Karakoram was presented by Desio (1979). A synthesis of the present-day crustal structure of the Karakoram inferred and interpreted from geophysical studies is presented by Molnar (this symposium).

Karakoram Plate and its boundaries

The Karakoram Plate extends from Afghanistan, through northern Pakistan and northern Ladakh to western Tibet (Desio 1964, 1980). Its boundaries are defined as the Rushan–Pshart Suture Zone within the southern Pamirs (Shvolman 1978) to the north, and the Shyok Suture Zone (SSZ), also referred to as the Northern Suture (Pudsey *et al.* 1985; Pudsey 1986; Coward *et al.* 1982, 1986, 1987), to the south. The western limit of the Karakoram Plate is not precisely known but it extends into the Hindu Kush Range of eastern Afghanistan (Tapponnier *et al.* 1981). Along the southern boundary of the central Karakoram, the SSZ structures have been reactivated by a major late Tertiary breakback thrust, the Main Karakoram Thrust (Searle *et al.* 1988). The MKT is largely responsible for the uplift of the mid- and lower-crustal rocks of the southern Karakoram. Within the Karakoram Plate, a major dextral strike-slip fault, the Karakoram Fault, shows approximately 150 km of right-lateral offset (Molnar &

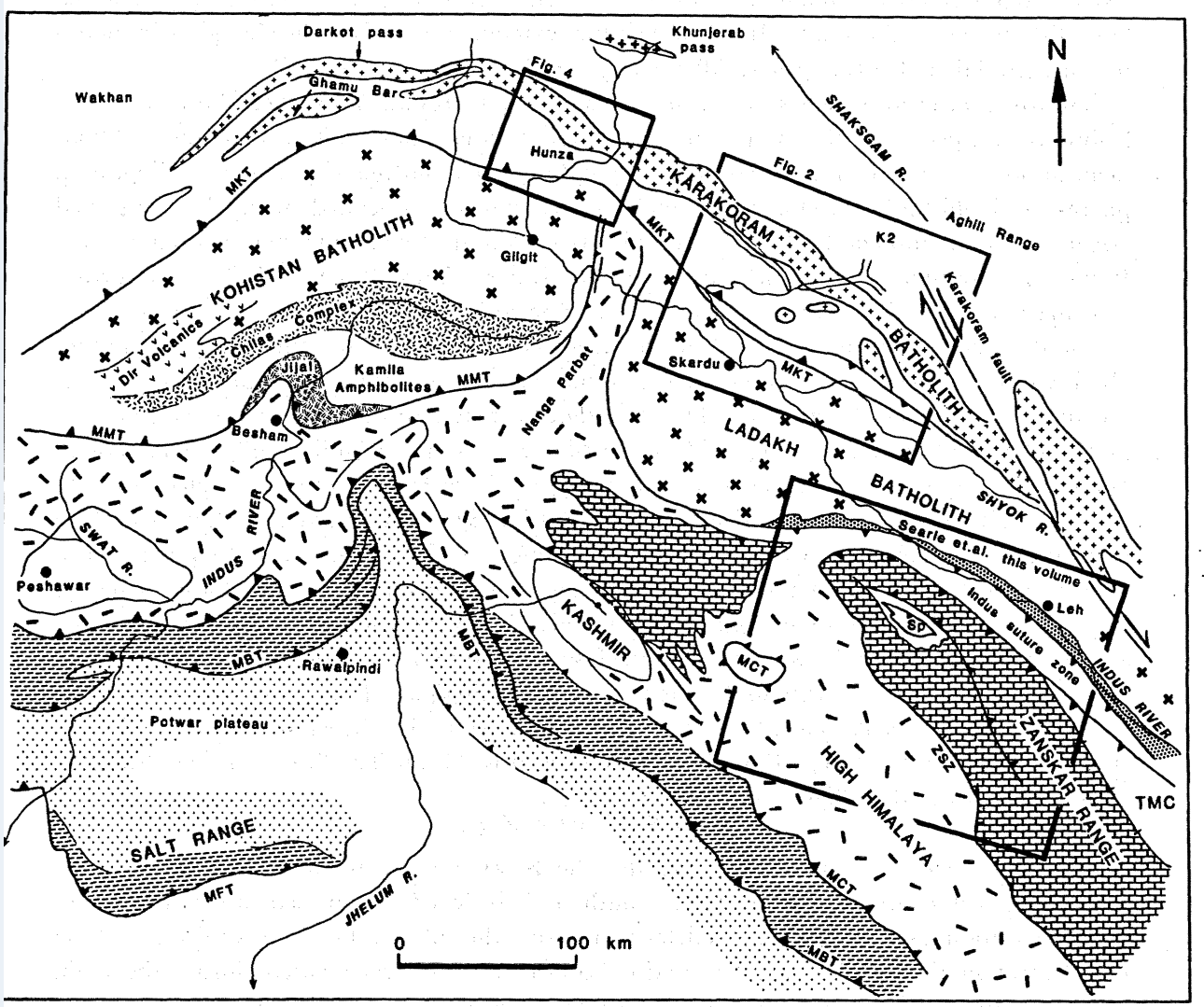

FIGURE 1. Simplified geological map of the western Himalaya–Karakoram showing the central Karakoram region discussed in this paper and the Ladakh–Zanskar Himalaya described by Searle *et al.* (this symposium). Abbreviations: MKT, Main Karakoram Thrust; MMT, Main Mantle Thrust; MCT, Main Central Thrust; MBT, Main Boundary Thrust; MFT, Main Frontal Thrust; Sp, Spontang ophiolite.

Tapponnier 1975). The stratigraphy and structure of the area remains poorly known and this paper is concerned mainly with the south-central part of the Karakoram Plate from the Hunza Valley in the west to the Hushe Valley in the east (figure 1).

Kohistan and Ladakh Terrane

The Kohistan–Ladakh Terrane, bounded to the north by the SSZ and to the south by the Main Mantle Thrust (MMT), is widely interpreted as a late Jurassic–Cretaceous island-arc. The Kohistan Terrane was first interpreted thus by Tahirkheli *et al.* (1979) and Bard *et al.* (1980). A synthesis of the geological history of Kohistan and its relations to regional collision tectonics is presented by Coward *et al.* (1986, 1987). A review of the Ladakh Terrane is presented by Searle *et al.* (this symposium). The two terranes are separated by the Nanga

Parbat Syntaxis about which the MMT is folded (figure 1). The Kohistan and Ladakh batholiths belong to the Trans-Himalaya belt that extends eastwards to the Gangdese batholith in southern Tibet (Gansser 1964; Allègre *et al.* 1984; Debon *et al.* 1986*b*).

Coward *et al.* (1986) suggest a two-stage history for Kohistan; an earlier phase of growth before SSZ closure in the mid-Cretaceous and a later phase following closure. Major deformation associated with the closure of the SSZ involved south-facing isoclinal folding. Both phases of Kohistan's development involved magmatism associated with the continued northward subduction of the Tethyan oceanic plate. Cessation of oceanic subduction due to the India–Asia collision resulted in closure of the Indus Suture Zone (MMT) and further deformation of the Kohistan sequence (crustal 'pop-up' structure; Coward *et al.* 1986).

The deepest part of the Kohistan arc sequence consists of high-pressure garnet granulites (Jijal–Patan Complex) and two-pyroxene granulites (Chilas Complex), interpreted as the sub-arc magma chamber. Related tonalitic and dioritic magmatism includes the Matum Das pluton with a Rb–Sr isochron age of 102 ± 12 Ma (Petterson & Windley 1985). The Kamila amphibolite sequence of metavolcanic and metaplutonic rocks has been interpreted either as oceanic crust precursory to the Kohistan arc (Bard 1983) or as the relics of an earlier arc (Coward *et al.* 1986). The overlying Chalt Volcanics and Yasin Group and equivalents in western Kohistan include early Cretaceous sediments and volcanics with typical arc chemistry.

Calc-alkaline magmatism led to the development of an Andean-type batholith following the accretion of Kohistan to the Karakoram and closure of the SSZ. Early basic dykes immediately post-date the SSZ closure, with main-stage plutonism taking place from uppermost Cretaceous to late Eocene times. A final phase of layered aplite-pegmatite sheets are Oligocene in age (Petterson & Windley 1985). Episodic magmatism in Kohistan therefore continued from the mid-Cretaceous to the Oligocene.

The Shyok Suture Zone

The Shyok Suture Zone (SSZ) separates the Karakoram Plate to the north from the Ladakh–Kohistan arc/microplate to the south. It is believed to represent a small back-arc basin depositional sequence that was deformed during the collision between Kohistan and the Karakoram in the mid-Cretaceous (Pudsey 1986) and later reactivated during the main collision with India. Rocks of the SSZ are strongly deformed and partly metamorphosed but consist of a mélange 150 m–4 km wide, containing blocks of volcanics, sediments and serpentinite in a slate matrix. Most of the blocks are derived from the Kohistan island-arc sequence to the south (Pudsey *et al.* 1985; Pudsey 1986).

Evidence for mid-Cretaceous closure of the SSZ includes: (*a*) Cretaceous volcanic rocks and Aptian–Albian limestones (Yasin Formation) are the youngest marine rocks in the SSZ (Pudsey 1986); (*b*) post-tectonic intrusions yield radiometric ages of 111–62 Ma, and a diorite dyke that cuts deformed volcanics within the SSZ has an $^{39}Ar/^{40}Ar$ age of 75 Ma (Petterson & Windley 1985); (*c*) the earlier deformation phase in Kohistan is mid-Cretaceous (Coward *et al.* 1986); and (*d*) along the SSZ in northern Ladakh, Tertiary continental molasse similar to the Indus molasse of the Indus Suture Zone unconformably overlie the Mesozoic oceanic sediments (Thakur & Misra 1984).

PHILOSOPHICAL TRANSACTIONS OF THE ROYAL SOCIETY A MATHEMATICAL, PHYSICAL & ENGINEERING SCIENCES

The central Karakoram

Within the central Karakoram three geologically distinct zones are recognized.

(i) *The Karakoram metamorphic complex*

The metamorphosed sediments and igneous rocks north of the MKT and SSZ, and south of the Karakoram batholith (the Karakoram metamorphic complex) have been divided into a number of lithological units (Desio 1964, 1979; Bertrand & Debon 1986; Searle *et al.* 1988). These units include dominantly metasedimentary sequences (Dumordo, Ganschen and Hunza schist units), felsic gneisses (Dassu gneiss) and migmatites and a prominent mélange that includes ultramafic rock (Panmah ultramafic unit).

(ii) *The Karakoram batholith*

The Karakoram batholith is now recognized as a composite magmatic belt following the reconnaissance work of Desio *et al.* (1964), Desio & Zanettin (1970) and Desio & Martina (1972). Recent geochemical, isotopic and geochronological determinations in the central Karakoram have resulted from studies along the Hunza Valley (LeFort *et al.* 1983; Debon *et al.* 1987; this paper) and in the Baltoro–Hushe region (Bertrand & Debon 1986; Searle *et al.* 1987, 1988). Magmatism evolved from pre-collisional, subduction-related to post-collisional types (Debon *et al.* 1987; Searle *et al.* 1988), with the prevailing tectonic environment strongly influencing petrogenetic processes and magma characteristics.

Episodic magmatism over a period of at least 80 Ma has been confined to the Karakoram batholith, which extends for over 600 km but reaches maximum widths of only 30 km. Such localization of magmatism implies that this narrow belt constitutes a major crustal lineament, which we refer to here as the Karakoram Batholith Lineament (KBL).

(iii) *The northern Karakoram Terrane*

Carboniferous to Jurassic (or possibly Lower Cretaceous) sediments constituting the Broad Peak and Gasherbrum Ranges north of the BPU (figure 2) are described by Desio (1964, 1979), Desio & Zanettin (1970) and Searle *et al.* (1988). The Gasherbrum sedimentary succession includes Carboniferous black shales that are overlain by a thick Permian and Mesozoic carbonate sequence with interbedded conglomerate, shale and tuffaceous horizons. Quartz diorites of the Broad Peak Porphyry unit intrude the sediments in the Broad Peak and Gasherbrum IV region (Desio & Zanettin 1970; Searle *et al.* 1988). The K2 area comprises interbanded ortho- and para-gneisses interpreted as mid-crustal rocks uplifted along the hangingwall of a major structural culmination (Searle *et al.* 1988). A sample of K2 Gneiss yielded a U–Pb date of 115 ± 3 Ma (R. Parrish, personal communication) and two other samples have K–Ar (Hbl.) ages of 111 and 94 ± 3 Ma (figure 2). Cross-cutting leucogranitic pegmatites have K–Ar ages ranging between 70 to 58 Ma (Searle *et al.* 1988).

The pre-collisional evolution of the Karakoram

Before India–Asia collision, Carboniferous to Lower Cretaceous sedimentary and volcanic sequences were intruded by Jurassic and mid-Upper Cretaceous batholiths. Pre-collision magmatism is characterized by calc-alkaline to mildly subalkaline intrusives of dioritic to

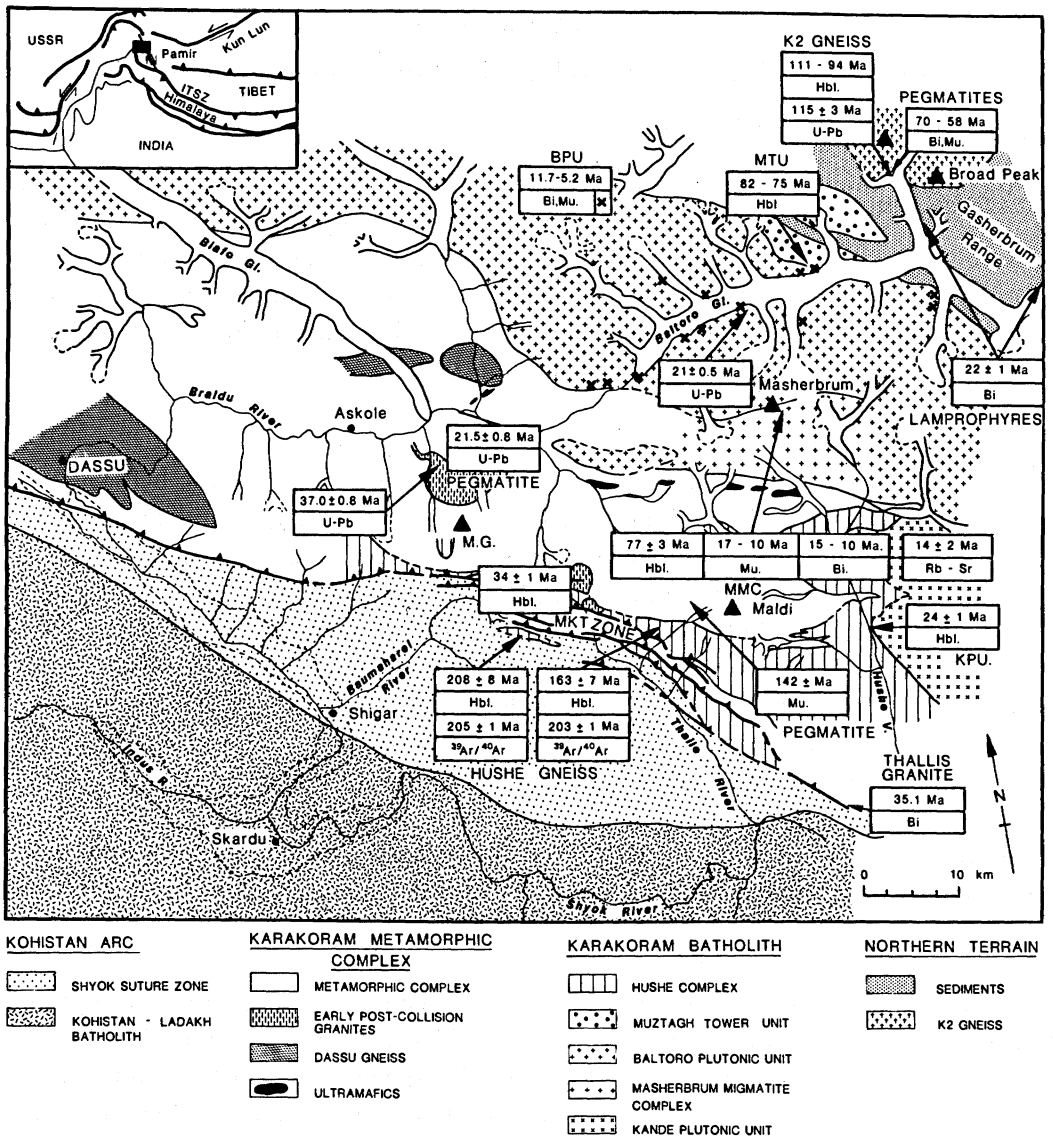

FIGURE 2. Simplified geology of the Baltoro–Hushe–Shigar region of the central Karakoram with radiometric age determinations for magmatic units. Hornblende (Hbl.), biotite (Bi.) and muscovite (Mu.) dates are all determined by K–Ar; data are listed fully in Searle *et al.* (1988). The black box in the inset map delineates the area within a regional context.

granodioritic composition. Mafic inclusions are typically observed and the granitoids are deformed and often recrystallized. Observations are consistent with reconstructions involving northward subduction of oceanic plate beneath the southern margin of the Karakoram Plate and voluminous subduction-related magmatism of Andean type. Magmas were preferentially emplaced into upper crustal levels along the Karakoram Batholith Lineament.

The Hushe complex

The oldest component of the Karakoram batholith, the Hushe complex, crops out south of the BPU along the Hushe Valley (figure 2). It is dominated by foliated orthogneisses

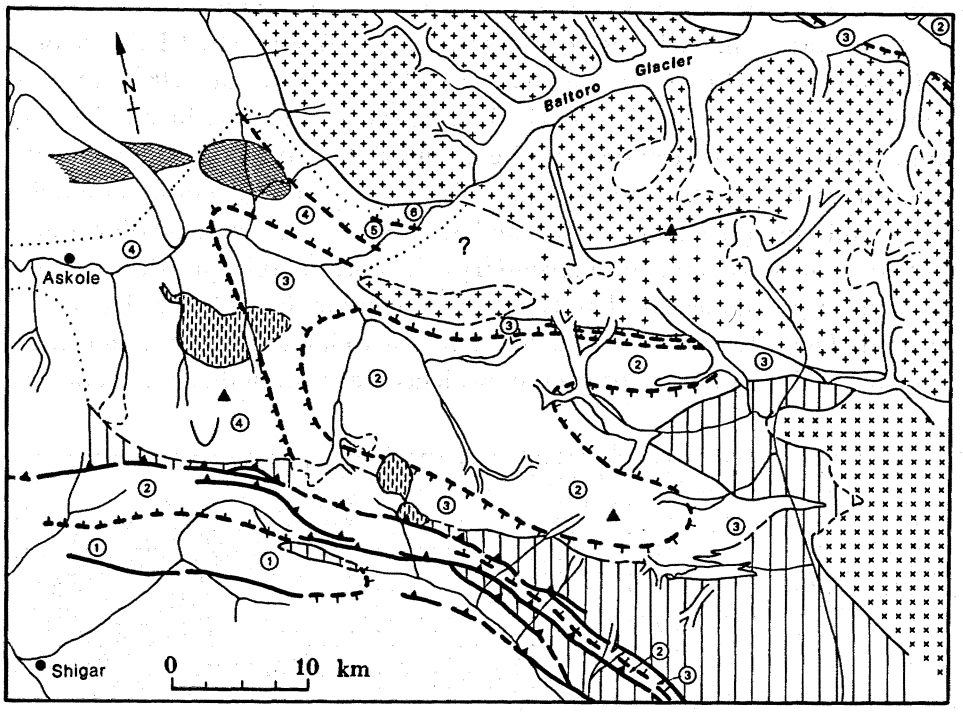

FIGURE 3. Map of the Baltoro–Hushe–Shigar region showing the distribution of metamorphic grades within the Karakoram metamorphic complex and sedimentary rocks of the northern Karakoram Terrane north of the Karakoram batholith. 1, very low grade, chlorite + white mica; 2, low grade, musc + Chl ± Chlt ± Bi ± Gnt; 3, staurolite grade; 4, kyanite grade; 5, sillimanite grade; 6, sillimanite grade with migmatites. Legend as for figure 2.

interlayered with minor amphibolites and felsic gneisses of granodioritic to monzogranitic composition. Jurassic ages of 208 ± 8 Ma and 163 ± 7 Ma (K–Ar; Hbl) pre-date cross-cutting monzogranitic pegmatite dykes with ages of 142 ± 6 Ma (K–Ar; Mu) and are supported by $^{39}Ar/^{40}Ar$ step heating analyses on two amphiboles showing minimum ages of 165 Ma and integrated ages of 205 ± 1.4 Ma and 203 ± 0.6 Ma. Although typically foliated and lacking any primary mineralogy and textures, the igneous character of the Hushe complex compels us to include it as an early component of the Karakoram batholith. The outcrop distribution of the Hushe complex suggests that it has been tectonically fragmented along south-directed thrusts within the MKT zone. The Hushe complex is spatially and temporally associated with a widespread low-pressure metamorphism (M1) in the area NE of the Thalle Valley (figure 3). Andalusite, staurolite and garnet-bearing pelitic assemblages (figure 6) are thought to represent the oldest metamorphic rocks in the area, associated with the Jurassic magmatic event (Searle *et al.* 1988).

The Hunza Plutonic Complex

The Hunza Valley segment of the Karakoram batholith is termed the Hunza Plutonic Complex (HPC). It encompasses at least three magmatic episodes and includes intricate, often diffusive, intrusions as well as well-defined leucogranitic bodies. Within the approximately 15 km wide HPC, semi-discrete zones of distinctive magmatism and broad north–south compositional gradients can be recognized.

The oldest component of the HPC, into which all younger magmas intrude, is a calc-alkaline

batholith (figure 4). A U–Pb age of 95±5 Ma from three samples of biotite–hornblende granodiorite (Le Fort *et al.* 1983) is corroborated by a 97±17 Ma Rb–Sr errorchron age (Debon *et al.* 1987). Mid-Cretaceous magmatism is also observed some 200 km west of Hunza where Debon *et al.* (1987) obtained a Rb–Sr isochron of 111±6 Ma on the Darkot Pass plutonic unit. There is a compositional gradient within the batholith with a general increase in acidity northwards. In the south, quartz diorites and mesocratic granodiorites are metaluminous and contain clinopyroxene and hornblende. Recrystallization during deformation resulted in the development of secondary minerals, notably euhedral epidote whereas primary minerals were annealed. Bands of gneiss contain hornblende-rich pods and are strongly sheared. The deformation affects the southern 10 km of the HPC. In contrast, at the northern contact of the batholith, peraluminous leucocratic granodiorites contain biotite. In

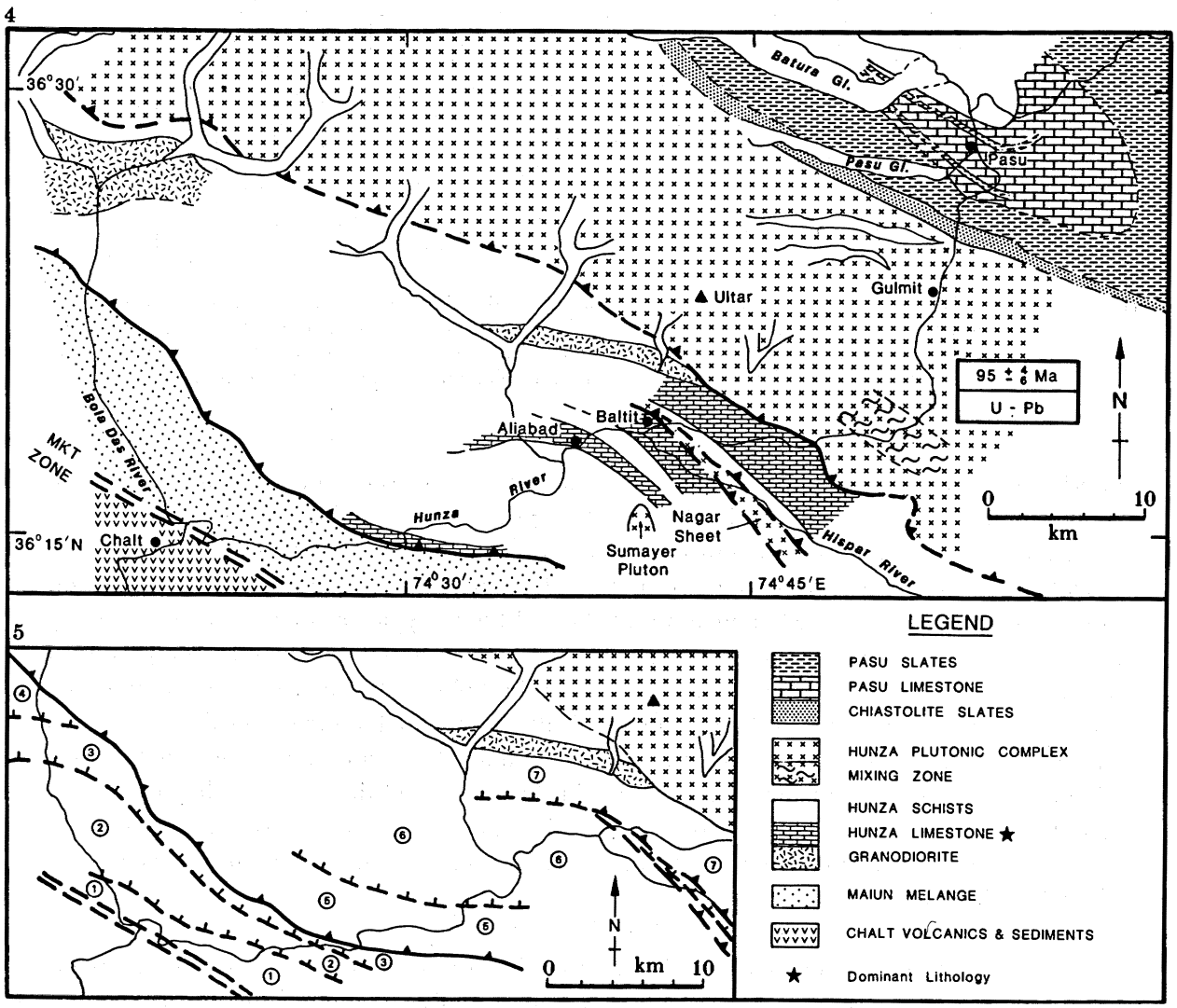

FIGURE 4. Geological map of the Hunza Valley region of the central Karakoram, with reliable radiometric data (from Le Fort *et al.* 1983).

FIGURE 5. Distribution of metamorphic grades in the Hunza Valley region. 1, Chtd+Bi+Chl; 2, Chtd+Gnt+Chl; 3, Gnt+Chl+Bi; 4, Gnt+Chl+Bi; 5, staurolite grade; 6, sillimanite grade; 7, migmatites.

the contact zone between the meta- and peraluminous granitoids they intercalate on scales between centimetres and sheets of 100 m or more. We therefore favour the intrusion of two separate plutons rather than the proposed magmatic differentiation model of Debon *et al.* (1987).

Within the deformed part of the HPC, approximately 1 km north of the southern contact, is a conspicuous mixing zone 2 km in width. Quartz diorites and granodiorites are associated with acidic and basic gneisses, plutons of acidic granodiorites and boudined leucogranitic sweats of pegmatite. Complex magma mixing processes and incipient migmatization were intimately involved in the development of the mixing zone. Aplitic sheets trending N–S emanate from the mixing zone and decrease in abundance away from each side of it. They are composed of biotite monzogranite with small inclusions of granodiorite.

Two generations of leucogranitic dykes can be recognized. The earlier ones are parallel to the foliation in the HPC, striking approximately east–west, and occur throughout the batholith. These are cut, folded and displaced by all other structures. The later ones are larger, more continuous sheets that transect all other structures including the southern contact of the HPC. They only occur in the deformed part of the batholith. Both igneous and metasedimentary inclusions are hosted by the early granitoids of the HPC and are confined to the marginal zones of the batholith.

The deformed southern and central part of the HPC has a distinct metamorphic foliation orientated about 135°/56° NE. It becomes indistinct northwards before changing to a southerly dip of about 100°/35° SSW. The two foliations can be interpreted as two discrete generations. The south-dipping structures to the north are associated with an intrusive contact parallel to the regional foliation of the country rocks (Pasu Slates). This contact is vertical or dips steeply south but not NE (Debon *et al.* 1987). The northward-dipping structures to the south, however, are parallel to the southern contact of the HPC, which shows clear evidence for post-emplacement thrusting. Therefore we suggest that the deformation and recrystallization, including the northward-dipping foliation, resulted from southward thrusting along the southern contact of the HPC, this foliation thus overprinting the primary intrusive foliation.

A second pre-collision magmatism in the Baltoro region is represented by the late Cretaceous Muztagh Tower Unit (MTU) (figure 2). Sheared biotite-bearing and hornblende-bearing tonalitic to granodioritic gneisses have K–Ar (Hbl.) ages of 82–75 ± 3 Ma (Searle *et al.* 1988). On the basis of compositional and age similarities, it is suggested that the MTU metagranitoids are the along-strike equivalents of the mid-Cretaceous intrusives of the HPC. Similary, the K2 gneiss (figure 2) has a U–Pb zircon age of 115 ± 3 Ma and is interpreted as belonging to the Karakoram batholith (Searle *et al.* 1988; R. Parrish, personal communication).

The geochemistry of the mid-Cretaceous magmatism

Both the Muztagh Tower Unit (MTU) and the Cretaceous component of the Hunza Plutonic Complex (HPC) display distinct calc-alkaline, subduction-related signatures typical of Andean-type tectonic settings. Representative analyses for these units are presented in table 1, although compositional ranges are very broad emphasizing the complex magmatic assemblages in the HPC. Granodioritic compositions are dominant within both of these units, typically with 60–70 % (by mass) SiO_2. On the normalized trace-element variation diagrams

(spidergrams; figure 8), the relative enrichments of Rb, Ba, Th, U and K (the large-ion lithophile elements, LILEs) and the negative Nb anomaly are characteristic of subduction-related magmas (Brown *et al.* 1984; Thompson *et al.* 1984). Absolute trace-element abundances are also compatible with typical continental subduction-related granitoids. The rare-earth element (REE) patterns (figure 9) indicate typical plagioclase + hornblende-dominated fractionation within the HPC to produce evolved patterns enriched in all trivalent REEs relative to the less evolved patterns, but with the progressive development of the characteristic negative europium (Eu) anomaly.

The pre-collision magmatic component of the Karakoram batholith is isotopically heterogeneous. Recent data indicate initial $^{87}Sr/^{86}Sr$ ratios of 0.705 to 0.713 on the HPC taking the 95 Ma zircon age as a model age. The least radiogenic end member is consistent with an initial $^{87}Sr/^{86}Sr$ ratio of 0.7044 for the Darkot Pass plutonic unit (111 ± 6 Ma; Debon *et al.* 1987). These values are typical of subduction-related magmas in continental environments. The range of initial $^{87}Sr/^{86}Sr$ ratios is not consistent with derivation from a single, homogeneous magma, even assuming that the model age of 95 Ma is applicable to all samples. The variation may result from differences in source composition or contamination. U–Pb ages on the Hushe and K2 gneiss suggest that both are deformed constituents of the Karakoram batholith that have inheritance and incorporation of older crustal material (R. Parrish, personal communication).

Evolution

The magmatic evolution of the Karakoram before India–Eurasia collision is partially paralleled in the Kohistan–Ladakh Terranes (figure 10). Mid-Cretaceous subduction-associated magmatism is observed both in the Karakoram batholith and the Kohistan–Ladakh batholiths. The contemporaneous activity is possibly related to a common northward-directed subduction zone. An alternative model (Debon *et al.* 1987) relates synchronous mid-Cretaceous magmatism to subduction of a 'southern Neotethys' south of Kohistan–Ladakh and parallel subduction of a 'northern Neotethys' south of the Karakoram. However, if the Kohistan–Ladakh Terranes have been correctly identified as island-arcs, with suture zones such as the SSZ representing ephemeral back-arc basins, such a model is considered untenable.

Accretion of the Kohistan–Ladakh Terranes with the Karakoram Plate at *ca.* 100–90 Ma (figure 10) is associated with observed folding and cleavage development in Kohistan (Coward *et al.* 1986). The Albian–Aptian Yasin Group limestones along the northern margin of Kohistan represent the latest marine sedimentation before accretion. The passive docking of the back-arc basin resulted in upright folding but no large-scale overthrusting. The SSZ has, however, been reactivated by breakback thrusting and strike-slip faulting after main ISZ closure (Coward *et al.* 1986).

Post-collisional evolution of the Karakoram

Timing of main collision between the Indian and the Ladakh–Kohistan–Karakoram Blocks along the ISZ is well constrained by palaeomagnetic (Klootwijk 1979; Patriat & Achache 1984), structural and sedimentological (Searle *et al.* 1987) data at *ca.* 50 Ma. East of the Nanga Parbat Syntaxis in Ladakh, the ISZ contains oceanic sediments and volcanics of Mesozoic–Lower Eocene age after which continental molasse deposition dominated. West of Nanga Parbat the ISZ (Main Mantle Thrust) places rocks of the Kohistan island-arc

PHILOSOPHICAL TRANSACTIONS OF THE ROYAL SOCIETY A MATHEMATICAL, PHYSICAL & ENGINEERING SCIENCES

TABLE 1. CHEMICAL ANALYSES OF REPRESENTATIVE ROCK TYPES FROM THE MAJOR PLUTONIC COMPLEXES AND UNITS OF THE CENTRAL KARAKORAM BATHOLITH

	1 B16	2 B9	3 B15	4 R42	5 R33	6 R35	7 R68	8 R11	9 SG2	10 SLV20	11
SiO_2	57.8	63.3	68.8	64.7	69.5	74.2	70.1	52.9	74.7	74.9	73.65
TiO_2	0.7	0.8	0.7	0.7	0.4	0.1	BD	1.6	0.1	BD	0.1
Al_2O_3	14.8	16.5	15.4	15.9	14.7	14.3	13.9	10.3	14.8	14.9	14.9
Fe_2O_3	7.2	5.4	4.4	5.4	2.1	1.0	1.1	6.9	0.9	0.5	0.8
MnO	0.1	0.1	0.1	0.1	BD	BD	0.4	0.1	BD	0.1	BD
MgO	5.1	2.7	1.3	2.4	0.7	0.1	BD	11.1	BD	BD	0.1
CaO	7.4	5.5	3.7	5.0	1.7	0.8	BD	6.0	0.8	0.9	0.5
Na_2O	3.0	3.0	2.8	2.9	4.0	3.9	4.3	1.1	4.2	4.7	4.05
K_2O	3.0	2.0	2.7	3.2	5.0	4.6	4.1	7.9	4.8	4.6	4.6
P_2O_5	0.2	0.2	0.2	0.1	0.2	0.1	0.1	1.7	0.1	BD	0.1
Ni	25	14	5	9	10	3	1	403	1	BD	< 10
Cr	179	51	19	60	23	16	12	580	BD	9	< 10
V	157	118	53	107	32	5	1.5	135	BD	BD	27
Zn	68	44	66	65	54	33	16	153	38	5	ND
Pb	24	19	21	26	92	46	22	106	60	82	ND
Cu	33	4	19	ND	4	5	4	ND	2	2	ND
Ga	18	15	29	21	20	22	27	19	26	16	ND
Rb	113	78	101	126	234	272	273	350	383	168	287
Sr	509	387	267	347	796	156	9	1221	41	86	76
Y	22	19	20	24	16	14	13	34	24	17	ND
Zr	97	148	206	182	244	71	30	692	40	17	43
Nb	12	10	14	14	22	21	21	46	16	6	ND
Ba	537	696	653	658	2317	442	10	3679	95	178	213
La	17	47	27	24	66*	20*	6*	114	10	2	6
Ce	34	84	56	46	141*	45*	20*	266	18	4	11
Nd	18	25.5	24	23	57*	18*	13.5*	136	9	2	5
Th	18	34	14	14	62	13	8	8	13	10	6
U	3	5	2.5	3	7	9	9	7	17	7	9

Locations: 1, Hunza Plutonic Complex; south contact; 2, Hunza Plutonic Complex; granodiorite; 3, Hunza Plutonic Complex; granodiorite, N. contact; 4, Muztagh Tower Unit; Hbl–Bi gneiss; 5, Baltoro Plutonic Unit; monzogranite; 6, Baltoro Plutonic Unit; leucogranite; 7, Baltoro Plutonic Unit; leucodyke; 8, Lamprophyre; Baltoro glacier; 9, Sumayar Pluton, Hunza; leucogranite; 10, Hunza Plutonic Complex; leucogranite dyke; 11, Average Manaslu granite, Nepal (Le Fort *et al.* 1987).

ND, not determined; BD, below detection limit; *, INAA data.

All internal data analysed by XRF techniques.

southwards on to the Indian Plate gneisses. After collision at 50 Ma, thrusting and crustal thickening propagated both south of the ISZ in the Zanskar and High Himalayan Ranges (Searle 1986; Searle *et al.*, this symposium) and north of the ISZ in the Karakoram. The regional metamorphism (M2) in the central Karakoram is related to post-collisional crustal thickening, largely by thrust stacking and/or homogeneous thickening (figure 11). An early post-collisional magmatism of Eocene–Oligocene age post-dates peak M2 metamorphism. Following a second magmatic gap late post-collisional magmatism occurred in response to major crustal thickening beneath the Karakoram.

Regional metamorphism, M2

The Karakoram metamorphic complex in the Hunza region is represented by two main units, the Hunza schists and the Maiun mélange, which are bounded to the south by the MKT and along the north by the Karakoram batholith (figure 4). In general terms, metamorphic grade in pelites and marbles increases northwards, and a pervasive foliation dips consistently NNE between 40 and 90°. The foliation is sub-parallel to bedding and shear sense indicators show thrusting towards the SSW. The two-dimensional isograd pattern shown in figure 5 is poorly constrained in three dimensions; it is suspected, but not proven that the metamorphism along the Hunza Valley is inverted (Coward *et al.* 1986). Mineralogical changes, usually parallel to foliation and bedding correlate with changes in bulk rock composition.

The phyllite matrix of the mélange includes chlorite–biotite–chloritoid and garnet-bearing assemblages. The highest grade assemblages in the mélange are andalusite-bearing and occur adjacent to the thrust contact with the Hunza schists. In pelitic lithologies within the Hunza schists, staurolite + garnet assemblages pass northwards into sillimanite + garnet assemblages and then into migmatites. In the more Ca-rich pelites and marbles, hornblende-bearing assemblages pass northwards into diopside-bearing marbles and close to the Karakoram batholith, plagioclase is replaced by scapolite. Maximum metamorphic conditions given by pelitic rocks close to the Karakoram batholith are 670 °C and 5 kbar† (Broughton *et al.* 1985). Snowball garnet and staurolite porphyroblast textures indicate that metamorphism was syn-tectonic (Powell & Vernon 1979; Prior 1987).

K–Ar biotite ages (D. C. Rex, unpublished data; Coward *et al.* 1986) young towards the region of highest metamorphic grade (figure 7). The andalusite hornfels of the Maiun mélange results from the tectonic uplift and juxtaposition of hotter garnet–staurolite schists along a major shear zone. The andalusite-forming reaction (garnet + chlorite = andalusite + biotite) occurs at about 400 °C, indicating that thrust uplift occurred close to the biotite K–Ar closure temperature. The biotite K–Ar ages can, in this case, be explained by syn- and post-metamorphic uplift on SSW-directed thrusts and shear zones that brought deeper and hotter rocks up in the north. These took longer to cool through the K–Ar closure temperature and give younger ages. Fission track ages do not vary across major tectonic contacts in the Hunza Valley (figure 7), suggesting that differential uplift occurring at moderately high temperatures (300–400 °C) had ceased by the time the area had cooled to 100–200 °C and uplift may have been occurring on one fault only. We correlate the main metamorphism in the Hunza Valley with M2 in the Baltoro region at *ca.* 45–36 Ma.

† 1 kbar = 10^8 Pa.

The northward-dipping foliations within the southern part of the HPC are parallel to the southern contact of the HPC, which shows clear evidence for post-metamorphic south-verging thrusting. We suggest that the deformation and recrystallization within the HPC, including the northward-dipping foliation, resulted from southward thrusting along the southern contact of the HPC, this foliation thus overprinting the primary intrusive foliation. The mixing zone developed at this time and localized melting resulted in the injection of aplitic sheet intrusions emanating from the mixing zone probably during the late Eocene–early Oligocene. Several north-dipping shear zones within the Hunza schists are probably related to this phase of crustal shortening. Syn-metamorphic deformation in the staurolite–garnet zones south of Aliabad (figure 5) therefore must be earlier than the post-metamorphic thrusting along the southern margin of the batholith to the north. This northward propagation of thrusting supports the contention that major crustal thickening processes in the Himalaya–Karakoram orogenic belt occurred by breakback thrusting propagating in the hangingwall of earlier thrusts (Searle *et al.*, this symposium; Hodges *et al.*, this symposium). Post-collisional magmatism in Hunza resulted in multi-stage leucogranite dyke injection and the emplacement of leucogranitic sheets and plutons at Sumayer and Nagar (figure 4).

In the Baltoro region, the main regional metamorphism is a high pressure-temperature Barrovian sequence, characterized by the assemblage kyanite–staurolite–biotite–garnet–muscovite–plagioclase–quartz (figures 3 and 6) with sillimanite–muscovite and sillimanite–K-feldspar assemblages locally developed (Searle *et al.* 1988). Within the Karakoram metamorphic complex there are isolated satellite plutons of early post-collision age (figure 2). The Mango Gusar two-mica granite has a U–Pb zircon date of 37.0 ± 0.8 Ma (R. Parrish, personal communication) and the Chingkang-la pyroxene–hornblende–biotite granite has a K–Ar (Hbl.) age of 34 ± 1 Ma (Searle *et al.* 1988).

The Baltoro Plutonic Unit

The Baltoro Plutonic Unit (BPU) is a batholith about 20 km wide and 80 km long (figure 2). It is restricted in composition to granitic and leucogranitic lithologies that are considered to be consanguinous. A well-defined U–Pb date of 21 ± 0.5 Ma on zircons from monzogranite samples reflects the crystallization age of the granite whereas monazite ages of 19–17 Ma reflect cooling through U–Pb closure temperatures of 650–700 °C (Parrish & Tirrul 1988). Eleven K–Ar (Bi.) dates reported by Searle *et al.* (1988) range between 12 and 5 ± 0.5 Ma on BPU granites and concur with an average age of 8.8 ± 0.3 Ma from three whole-rock–plagioclase–biotite internal isochrons (Debon *et al.* 1986). We interpret these dates as recording uplift and cooling events. Furthermore, the younging of K–Ar dates towards the margins of the BPU suggests fluid interaction effects between the granite and wallrock. The crystallization age of 21 Ma clearly refers the BPU to a late post-collisional intracontinental magmatism.

Although the BPU is compositionally restricted, three lithological groups are apparent. The monzogranites are the least evolved and contain plagioclase + K-feldspar + biotite + quartz ± muscovite, the latter being secondary; amphibole is very rare. Minor phases include apatite, sphene, zircon, allanite, monazite, thorite, tourmaline and opaques. The second group includes the two-mica ± garnet leucogranites and leucogranitic aplite and pegmatite dykes constitute the third group.

The southern margin of the BPU, south of the Baltoro glacier, is a migmatitic complex up

PHILOSOPHICAL TRANSACTIONS OF THE ROYAL SOCIETY A MATHEMATICAL, PHYSICAL & ENGINEERING SCIENCES

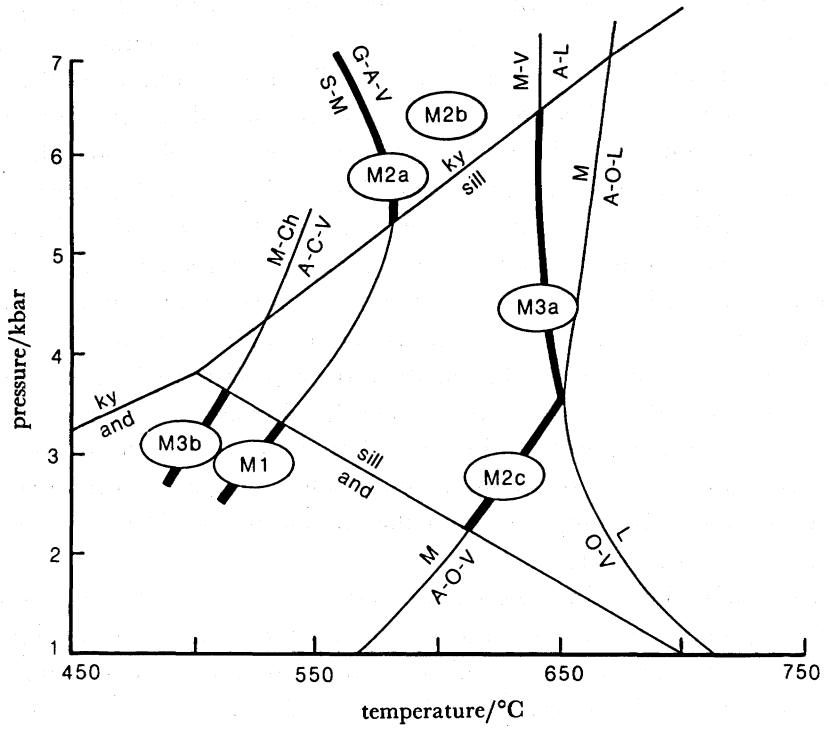

FIGURE 6. Pressure–temperature grid showing key assemblages observed in the Baltoro–Hushe Karakoram (from Searle *et al.* 1988). All assemblages contain biotite, hornblende and quartz. A, andalusite, kyanite or sillimanite; C, cordierite; Ch. chlorite; G, garnet; L, granitic liquid; M, muscovite; O, orthoclase; S, staurolite; V, vapour. (1 kbar = 10^8 Pa.)

to 10 km wide: the Masherbrum Migmatite Complex (MMC). Paragneisses, including calc-silicate marbles, orthogneiss, strongly deformed migmatite and penetrating granitic sheets are cross-cut by complex leucogranitic dyke swarms. A Rb–Sr whole-rock isochron on these yields an age of 14.1 ± 2 Ma with an $^{87}Sr/^{86}Sr$ initial ratio of 0.7084 (Searle *et al.* 1988). K-Ar (Bi., Mu.) determinations on various pegmatites, leucogranites and gneisses yield ages between 17 and 10 Ma. One K–Ar (Hbl.) age of 77 Ma on a schist is consistent with the interpretation that older components of the Karakoram batholith are represented as protolithic material in the MMC.

Spatially and temporally associated with the BPU are biotite–minette (lamprophyre) dykes. Three K–Ar (Bi.) dates (figure 2) of $24–22 \pm 1$ Ma suggest their emplacement immediately before the BPU at 21 ± 1 Ma. The dykes form a 'shadow-zone' about the BPU.

The intrusion of the Baltoro plutonic unit at 21 Ma superimposed a contact metamorphism (M3) on the low-grade sediments along the northern margin of the BPU (figure 3). Andalusite in the aureole at Mitre Peak constrains the pressure to less than 3.75 kbar (figure 6). The M3 imprint along the southern margin of the BPU is more controversial. Searle *et al.* (1988) noted an increase in temperature towards the granite contact within the M2 sequence with the successive disappearance of staurolite, the appearance of sillimanite and the development of granitic melt pods within migmatitic terrain. This increase in temperature could be attributed to the thermal effect of the granite superimposed on regional M2 metamorphism (see

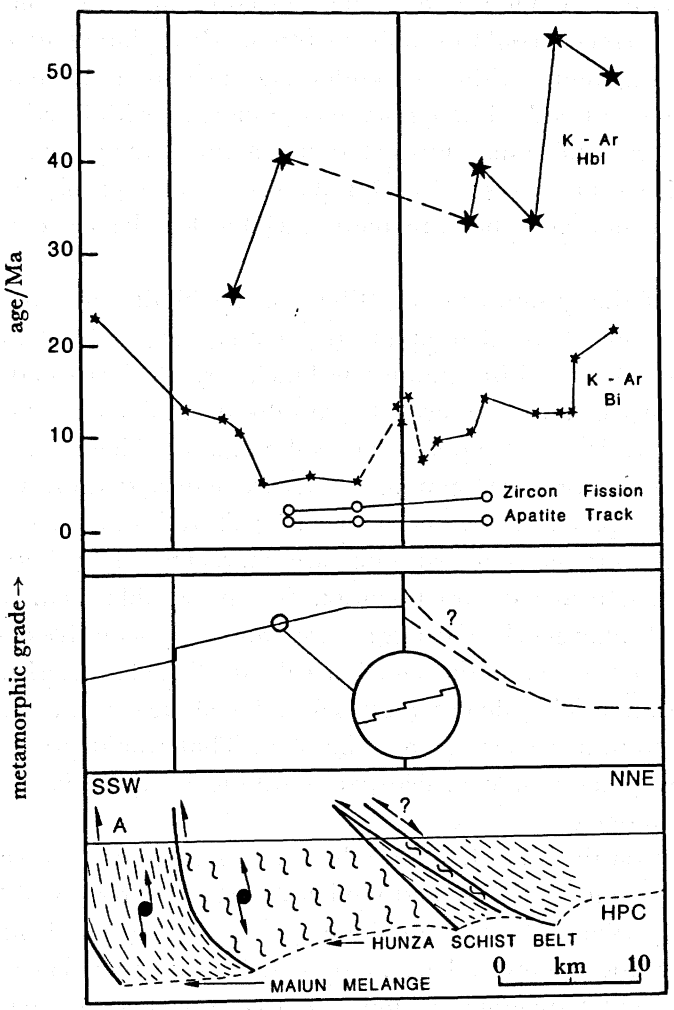

FIGURE 7. Schematic cross section through the Hunza Valley showing major tectonic boundaries, extent and general attitude of foliation and shear sense interpreted from macrostructural and some microstructural evidence. Metamorphic grade increases northwards and is shown schematically. Close-up of profile is to show that changes in metamorphic grade relate primarily to minor thrusts rather than a palaeo-geotherm. The upper part of the diagram shows K–Ar data of D. C. Rex (unpublished, and in Coward *et al.* 1986). Fission track data from Zeitler (1985). HBL., hornblende; BI., biotite; ZIR., zircon; AP., apatite.

Discussion). A leucogranite dyke cross-cutting this sequence approximately 10 km SW of the BPU has a U–Pb zircon age of 21.5±0.8 Ma (figure 2; R. Parrish, personal communication). Dyke emplacement within the migmatite terrane was therefore synchronous with emplacement of the BPU.

Geochemistry of the post-collisional Baltoro Plutonic Unit

The Baltoro Plutonic Unit is the largest and best documented post-collisional granite within the Karakoram batholith. Field observations and comprehensive geochemical data on over 50 representative samples allow lithological classification and subsequent modelling of geochemical evolution. Table 1 lists representative analyses for the different lithologies constituting the BPU.

The BPU is a mildly peraluminous and highly evolved granite intrusion with 68–75% (by mass) SiO_2. All major elements conform to linear trends when plotted against a fractionation index, indicating consanguinuity within the pluton and a common magma evolution. K_2O is exceptional in revealing no trend, although an overall increase with fractionation is observed. This is attributed to its remobilization during late-magmatic K-metasomatism associated with the growth of K-feldspar megacrysts. Na_2O/K_2O ratios are typically around one for the monzogranites and leucogranites but are more variable for the leucogranitic aplites and pegmatites.

The least evolved of the granites in the BPU are the biotite monzogranites. These are unusually enriched in Ba (315–2300 p.p.m. (by mass), avg. = 1100 p.p.m., $n = 28$), Sr (100–800 p.p.m (by mass), avg. = 515 p.p.m.) and the REEs. The heat-producing elements, K, Th and U, are also enriched with respect to crustally derived melts (Th: 5–85 p.p.m. (by mass), avg. = 23 p.p.m.; U: 1–11 p.p.m., avg. = 4.5 p.p.m.) whereas Rb tends to be low (90–260 p.p.m. (by mass); avg. = 160 p.p.m.). Trace element spidergrams (figure 8) illustrate pronounced positive Th spikes, positive normalized U/Th ratios and negative spikes for Nb, P and Ti. REE patterns for the monzogranites are characterised by both strong light REE enrichment and light REE/heavy REE fractionation. No appreciable Eu anomaly is developed.

The monzogranites display geochemical signatures most representative of the magma source being the least evolved component of the BPU. The calc-alkaline characteristics of the BPU must be inherited from the source. They do not imply derivation of the BPU as a high-level, physically separated fractionate from a deeper magma chamber. That would produce a fractionation pattern dominated by precipitation of feldspar, resulting in appreciable Sr depletion and development of a Eu anomaly.

All the leucogranites on the other hand are depleted throughout in trace elements relative to the monzogranites except for Rb, K and the heavy REEs (figures 8 and 9). This depletion does not appear to represent source composition but rather high-level magmatic processes. Likewise, the leucogranitic aplites and pegmatites show wide chemical variation reflecting extreme fractionation and late-magmatic, fluid-enhanced processes. Differentiation of the melt through some fractionation process can account for the observed elemental depletions during magma evolution. In particular, Ba and Sr are removed in feldspar and biotite and P, (Zr) and Ti by apatite, (zircon) and sphene respectively. The spectacular depletion in the light REEs from monzogranites to evolved differentiates, whereas HREE abundances remain fairly stable, is attributed to monazite (& allanite?) control, although feldspar will also be effective. Monazite (and thorite?) fractionation is also responsible for changing the normalized U/Th ratio from less than 1 in the monzogranites to more than 1 in the leucogranites. Uranium thus behaves more incompatibly than Th throughout magma evolution (partition coefficient data for quantitative geochemical modelling from Arth 1976, Hanson 1978 and Henderson (ed.) 1984).

Initial $^{87}Sr/^{86}Sr$ ratios for the BPU vary between 0.7072 and 0.7128. Preliminary data on whole rocks indicate that oxygen isotope compositions are uniformly heavy, in the range 9.6–11.2 ‰. The isotopic characteristics of the BPU are considered to reflect the isotopic composition of the source region except where exchange has taken place close to the granite contact. Strontium and oxygen isotopic compositions are appreciably lower than those of the High Himalayan post-collisional leucogranites that exceed 0.730 (at 20 Ma) and 11.0, respectively (Deniel *et al.* 1987; Le Fort *et al.* 1987).

PHILOSOPHICAL TRANSACTIONS OF THE ROYAL SOCIETY A MATHEMATICAL, PHYSICAL & ENGINEERING SCIENCES

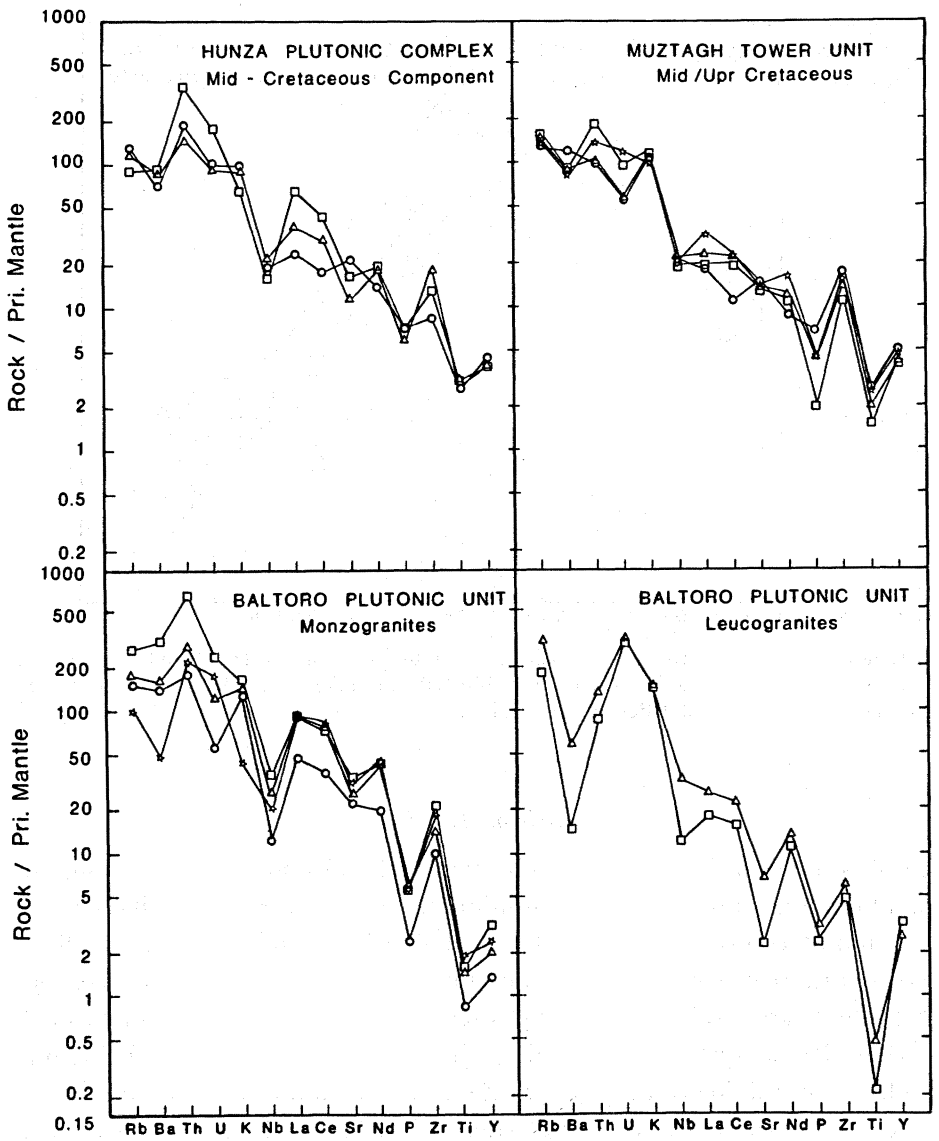

FIGURE 8. Primordial-mantle normalized trace element variation diagrams (spidergrams) for pre-collision (HPC and MTU) and post-collision (BPU) components of the Karakoram batholith.

The lamprophyres that are spatially and temporally associated with the BPU are extraordinarily enriched in most trace elements (table 1) with overall geochemical signatures displaying some similarities to the BPU. Compared to other late tectonic to post-tectonic calc-alkaline lamprophyres, however (Rock 1984; P. Henney, personal communication), they show similar elemental abundances. Of particular interest are the high concentrations of K_2O, Sr, Ba, Th, U and the light REES, just the elements that are anomalously enriched in the BPU granites. A primary continental mantle lithosphere source is envisaged for the lamprophyres; concentrations of refractory elements such as V, Ni, Cr preclude a crustal derivation (Rock 1984; Foley *et al.* 1987). However, a component derived from subducted continental crust is possible (see Discussion).

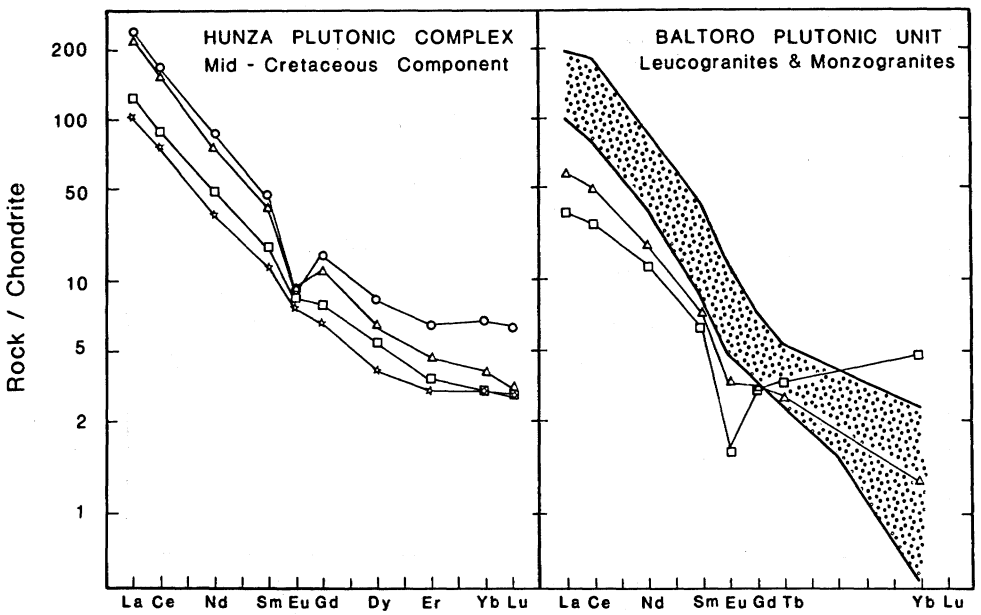

FIGURE 9. Chondrite-normalized rare-earth element (REE) patterns for pre-collision (HPC) and post-collision (BPU) components of the Karakoram batholith. REE data for the HPC are taken from Debon *et al.* 1987. The stipple represents the REE envelope for four BPU monzogranites.

Petrogenesis of the BPU

The BPU consists of an evolved granitic suite that lacks an observed basic component. Its mineralogy, peraluminous affinity and near-minimum melt composition all indicate a crustal derivation. The almost complete absence of tourmaline is diagnostic of a volatile-depleted magma and corroborates geochemical evidence for a relatively anhydrous melt source. In particular, Rb contents are lower than other post-collision granites such as Manaslu (Le Fort 1981). This has high Rb, consistent with melting of continental crust that was being infiltrated by migrating Rb-bearing fluids during dehydration and metamorphism (Vidal *et al.* 1982). Although the BPU is interpreted as a crustally-derived melt (Searle *et al.* 1988), enclaves are rare and confined to the pluton margins (xenoliths). However, rare xenocrystic sillimanite within monzogranite, breaking down to produce K-feldspar and muscovite under K-rich fluid fluxing, implies a metasedimentary component to the source. In addition, a large inherited component to the zircons suggests a protolith heterogeneous in primary age and hence of a hybrid source. These source ages range from 600–500 Ma to older than 1700 Ma (Parrish & Tirrul 1988).

Further evidence suggests that a major source component for the BPU was dominantly quartzo-feldspathic. Likely bulk compositions include immature quartzo-feldspathic meta-pelites, volcaniclastics and orthogneisses. These are generally relatively depleted in Rb, thus yielding a melt with low Rb and unradiogenic initial $^{87}Sr/^{86}Sr$ ratios. They would also be expected to provide moderate $\delta^{18}O$ values. At high (granulite facies) P–T conditions, dehydration melting (mainly biotite) in the source would produce a granitic melt, deficient in included restite (Clemens & Wall 1981; Clemens & Vielzeuf 1987). Retention of garnet in

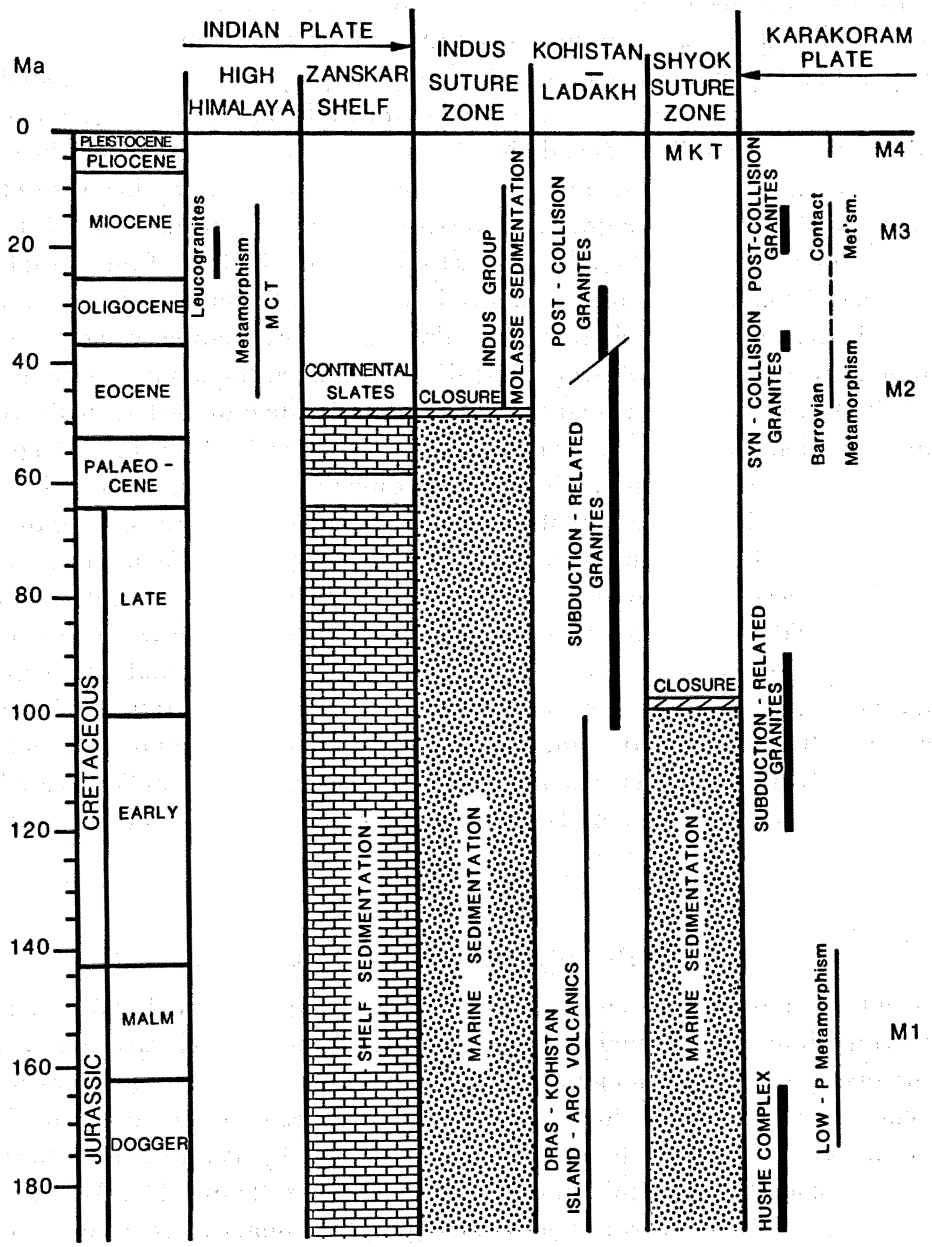

FIGURE 10. Simplified space-time chart based on radiometric ages for Kohistan–Ladakh and the Karakoram presented in Searle *et al.* (1988).

the residue may help to explain the heavy REE depletion in BPU monzogranites. The amount of melt required before a magma forms and begins to migrate (the critical melt fraction: CMF) is dependent mainly upon the temperature and water content of the melt and the restite content of the magma. Although the CMF is in much debate at deep crustal levels (see Wickham 1987; Clemens & Vielzeuf 1987; Rutter & Wyllie 1988), it is considered that, in fluid-absent conditions, the introduction of hot material in or adjacent to the potential melting site is a likely

candidate to promote sufficient melting. The lamprophyres observed in the vicinity of the BPU may offer an explanation for the localized conditions required for melt production.

The temporal and spatial association between the lamprophyres and BPU complies with a globally observed lamprophyre – post-collisional granite relation (Rock 1984; Thompson *et al.* 1984). This association implies a genetic link related to specific mantle conditions in a post-oceanic subduction, crustal thickening environment. The unusual geochemistry of the BPU compared to other post-collisional granites (Harris *et al.* 1986), particularly the high K, Ba, Sr, LREE, U and Th contents, may be related to selective contamination of the crustal source by a volatile-enriched fluid, or a magma genetically related to the lamprophyre mantle source. Fluids derived from the lamprophyre melt in the lithospheric mantle would be enriched in incompatible elements because of strong partitioning between the lamprophyric magma and the fluid. A fluid with such a high volatile content may migrate into the base of the continental crust as an emanation precursory to the main extraction of lamprophyric melt. To produce the required incompatible element-enriched liquid directly from unmodified lamprophyric magma, however, would require crystallization and removal of a refractory residue from the magma. Infiltration of such a high-temperature liquid into the thickened continental crust would provide the necessary heat, as well as geochemically modifying the BPU source region. Rapid melting would ensue, primarily through very rapid heating above ambient conditions. The age relations between the BPU (21 Ma crystallization age) and the lamprophyres (24–22 Ma late crystallization age) is consistent with rapid migration of the primary lamprophyric melt into the mid-crust, and a lag period for generation and migration of the BPU magma body. Its emplacement would take place some few million years later. The tectonic implications for such a post-collisional petrogenetic model are presented in the Discussion.

Discussion

Post-collisional tectonic evolution

The present-day crustal thickness of the Karakoram is approximately 65–70 km (Molnar 1984; this symposium) and yet middle to lower crustal rocks of the Karakoram metamorphic complex are presently exposed along the southern part of the Karakoram Plate. Structural and metamorphic constraints show that regional metamorphism in the southern Karakoram occurred from *ca.* 45–36 Ma with subsequent exhumation by south-directed thrusting and concomitant erosion during continuing crustal thickening (figure 11). We propose that deformation and uplift of the Karakoram metamorphic complex occurred in response to underthrusting of the leading edge of the Indian Plate beneath Kohistan and the southern part of the Karakoram (figure 11). Coward & Butler (1985) and Coward *et al.* (1986, 1987) record 470 km of shortening from the MMT to the Pakistan foreland in Indian Plate rocks, and argue for large-scale underthrusting of Indian lower crust northwards as far as the Pamirs. From shortening estimates of the Zanskar, Ladakh and Kashmir Himalaya, Searle *et al.* (this symposium) argue for underthrusting of Indian lower crust northwards as far as the Karakoram batholith but not beneath the Pamirs and Tibet.

The timing of metamorphism and deformation is constrained by undeformed granite intrusions that cross-cut the syn-metamorphic foliation, and have ages of 36–34 Ma (Searle *et al.* 1988). Along the Hunza Valley, syn-metamorphic south-directed thrusting, which may

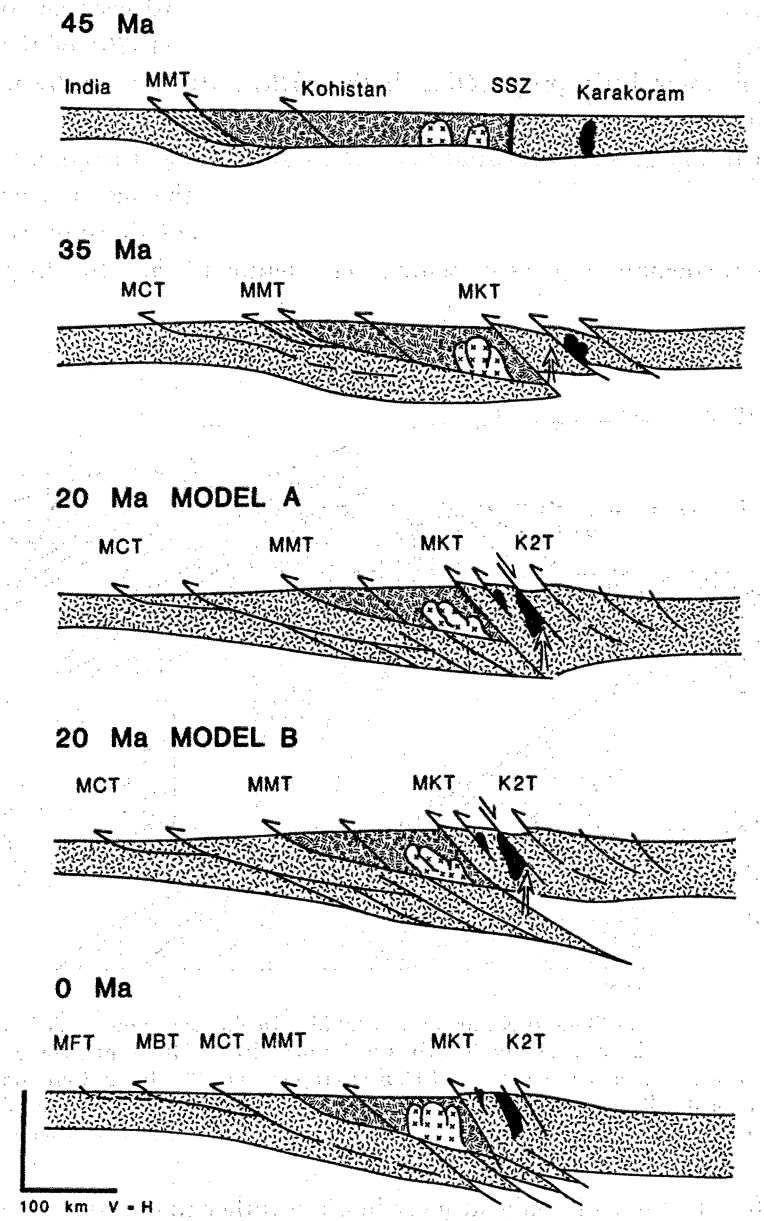

FIGURE 11. Schematic crustal profiles through the northern Indian, Kohistan and Karakoram Plates to illustrate the post-collisional evolution of the Karakoram. At 20 Ma two models are presented, model A being simple homogeneous thickening and model B crust–mantle imbrication. Abbreviations: K2T, K2 Thrust; MKT, Main Karakoram Thrust; MMT, Main Mantle Thrust; MCT, Main Central Thrust; MBT, Main Boundary Thrust; MFT, Main Frontal Thrust.

have been responsible for inverting the metamorphic isograds within the Hunza schists, propagated northwards to post-metamorphic thrusting along the southern margin of the Karakoram batholith. M2 metamorphism in the Karakoram is broadly synchronous with High Himalayan metamorphism to the south (Oligocene-Miocene; see Searle *et al.*, this symposium). We can therefore demonstrate that crustal thickening and regional metamorphism were occurring both in the Himalaya and the Karakoram following closure of the

ISZ. The out-of-sequence thrusting with respect to the southward vergence observed in the Hunza Karakoram supports the model of England & Searle (1986) of thrusting, crustal thickening and metamorphism propagating both northwards and southwards of the ISZ following collision.

Geochronological and geochemical studies on the post-collisional magmatism in the early Miocene, with metamorphic observations, further constrain the tectonic evolution of the Karakoram at this time. These constraints only apply fully to the Baltoro transect through the Karakoram, so the schematic models presented here (figure 12) are directly relevant to this area.

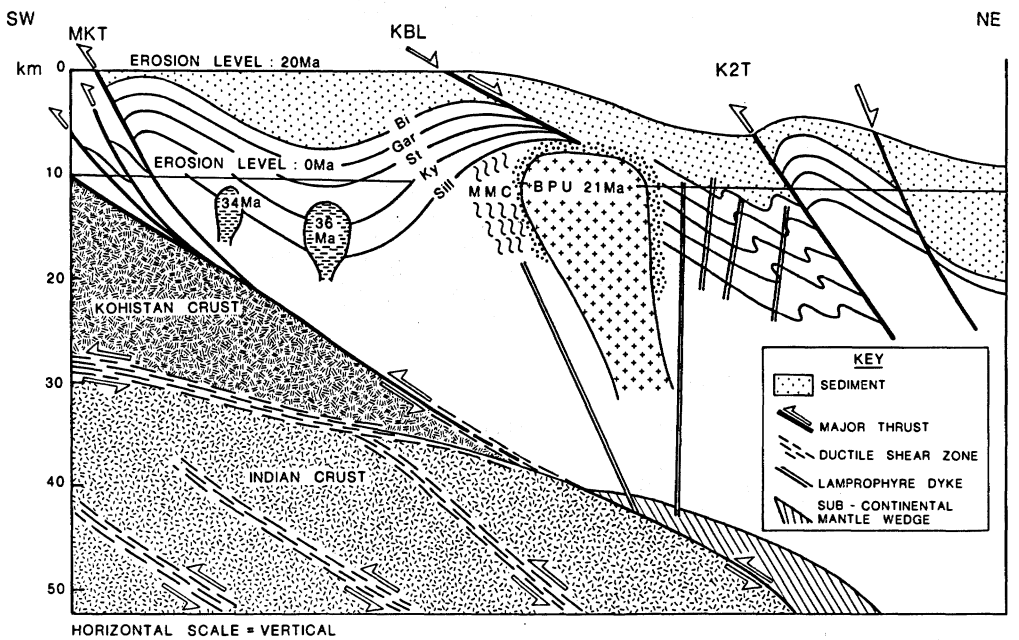

FIGURE 12. Thermal model for the Baltoro Karakoram at 20 Ma. In this schematic, scaled crustal section, M2 metamorphic isograds are illustrated as both perturbed by the effects of BPU intrusion at 21 Ma and offset along the MKT zone. The model assumes *ca.* 10 km of erosion since 20 Ma, and erosion levels are shown schematically. Major ductile shear zones bound Kohistan, Indian and Karakoram crustal blocks and basal detachments of the latter two are considered to flatten with depth. See text for discussion.

A most important feature, still only strongly inferred rather than positively observed, is the Karakoram Batholith Lineament. As stated earlier, this has been the site of magmatic activity at least since the mid-Cretaceous (or even the Jurassic if the Hushe complex is a tectonically fragmented component) until the mid-Miocene. The KBL was reactivated during and for some time before the mid-Miocene as a normal fault, downthrowing north. We suspect that culmination-collapse was initiated in response to crustal thickening beneath the Karakoram and resultant uplift of the Karakoram metamorphic complex. The mid-Miocene intrusion of the BPU into mid-crustal levels, estimated from the M3 aureole assemblages at around 12–15 km (Searle *et al.* 1988), is compatible with an extensional régime in the mid-upper crust along the lineament. Magma was tapped along deep crustal structures, probably ductile shear zones, and directed into the mid-crust along the footwall of the KBL.

Extension along the KBL before and during emplacement of the BPU is required to

juxtapose medium- to high-grade metamorphic terrain south of the Karakoram batholith against low-grade sediments to the north, both superimposed by M3. This is seen both in the Hunza section and in the Baltoro. Considerable uplift of the southern crustal block is therefore required; it is proposed that movement occurred along the MKT to the south and the KBL to the north. If steady-state uplift took place following 10 Ma of crustal thickening after main collision at 50–45 Ma, an estimated uplift rate of 1 mm a^{-1} is required before intrusion of the BPU. The uplift of the M2 sequence then complies well with the early post-collisional granites, intruded at 36–34 Ma, cross-cutting the regional M2 fabric (figure 12). Barrovian metamorphism would therefore post-date crustal thickening after collision and pre-date the lowest Oligocene granites (therefore, *ca.* 40–36 Ma).

Post-collisional thermal evolution

With post-M2 displacement along the KBL before intrusion of the BPU, low-temperature sedimentary rocks to the north were juxtaposed against hotter medium- to high-grade metamorphic rocks to the south. The tectonic juxtaposing of rocks of different metamorphic grade but otherwise identical characteristics will result in the downwarping of isotherm surfaces on the upthrow side and vice versa, with lateral heat transfer due to thermal disequilibration (Harte & Dempster 1987). The lower thermal conductivity of sedimentary rocks over crystalline rocks, gneisses and granites would promote a conductivity contrast, envisaged by Pinet & Jaupart (1987) to be intimately associated with the petrogenesis of the High Himalayan granites and their localization at corresponding structural positions. Sedimentary rocks north of the KBL would thus have acted as a barrier to lateral heat transfer (Jaupart & Provost 1985).

It is therefore significant that the BPU should be emplaced along the footwall of the KBL where a horizontal temperature maximum is localized, as this would be a further inhibitor to magma cooling. The BPU could thus migrate higher in the crust because of the low water content of the melt as a consequence of biotite-dominated dehydration partial melting, to the KBL acting as a magma conduit, to an extensional régime in the mid-upper crust and to the localized temperature anomaly imposed by the thermal contrast effect.

We suggest that the combination of emplacement of the BPU and the thermal effect across the KBL was responsible for the extensive M3 thermal metamorphism in the Karakoram metamorphic complex. Assemblages including garnet + biotite + muscovite + quartz + plagioclase + sillimanite + melt are developed within migmatitic terrane (Searle *et al.* 1988) so migmatization is considered an *in situ* development, with the associated leucosome melts genetically unrelated to the BPU melt.

The prevailing crustal framework (figure 11) has important implications for the source region of the BPU and the lamprophyres. Essentially, a simple homogeneous thickening model (figure 11; 20 Ma model A) for the deep structure of the Karakoram would necessitate vertical migration of melt through an estimated 50–60 km of continental crust. However, the crust–mantle imbrication model (figure 11; 20 Ma model B), whereby a mantle wedge separated Karakoram crust from Indian crust, would permit melting near to the base of the Karakoram crust to produce the BPU magma, the mantle wedge constituting a likely source for the lamprophyres. The relatively young, hot continental lithospheric mantle may have been enriched through devolatilization and dehydration in the subducting Indian crust. The

resultant melts would only have to migrate a maximum of 30 km through the Karakoram crust.

The Karakoram: an analogue to the High Himalaya?

Finally, we note a parallel in several temporal and structural processes between the Karakoram and the High Himalaya. The Barrovian metamorphism observed in both regions, within structurally bound blocks, is probably coeval and related to crustal thickening propagating both northwards and southwards from the ISZ. Uplift and exposure of the high-grade metamorphic terrane occurred along the MKT north of the ISZ and along the Main Central Thrust (MCT) to the south; both structures acting as south-directed thrusts. In response to crustal thickening and uplift of crustal blocks, dorsal culmination collapse occurred at high levels along the inferred KBL in the Karakoram (Searle *et al.* 1988) and along the Zanskar Shear Zone north of the High Himalaya (Burg *et al.* 1984*a*, *b*; Burchfield & Royden 1985; Searle 1986; Hodges *et al.*, this symposium). Juxtaposition of high-grade metamorphic terrane against Tethyan sediments in Zanskar is estimated to have involved a vertical displacement of *ca.* 19 km (Herren 1987).

A significant difference between the Karakoram and the High Himalaya is the composition and source of the leucogranites and their genesis. The anatectic, often 'minimum-melt', leucogranites of the High Himalaya were generated more or less *in situ*, and a number of petrogenetic models have been proposed (see Hodges *et al.*, this symposium). The Miocene post-collisional granites in the Karakoram, however, were generated in a deeper, more anhydrous region of the crust. The melt zone corresponds more or less to our estimate of the northernmost limit of underplating of the Indian crust. Our petrogenetic interpretation of the BPU is primarily based on petrographic, geochemical and isotopic evidence. Tectonic, thermal and structural considerations have also been integrated to produce an overall schematic model (figure 12). In particular, the lower initial $^{87}Sr/^{86}Sr$ ratios and $\delta^{18}O$ values for the BPU relative to leucogranites of the High Himalaya suggest a source fundamentally different from the mainly metasedimentary compositions that comprise the Karakoram metamorphic complex and the Central Crystalline Complex. Further, the absence of volatiles together with evidence for dehydration melting is consistent with a deep crustal source where contamination by a mantle-derived component is a realistic proposition.

A.J.R. and M.P.S. acknowledge NERC grant GR3/4242 to B. F. Windley and also a Royal Society grant (1985) and additional funding from the Mount Everest Foundation. D.C.R. acknowledges NERC grant GR/5932; M.B.C., grant GT4/85/GS/47; and D.J.P., NERC grant GT/83/GS/117. We thank Brian Windley, Paul Hoffman, Marc St Onge, Patrick Le Fort and Paul Henney for discussions, Randy Parrish for permission to quote unpublished U–Pb dates and Andy Saunders for critically reviewing earlier versions of the manuscript. Our thanks to Sue Button for producing an excellent set of slides for the symposium and diagrams in this paper.

References

Allègre, C. J. *et al.* 1984 *Nature, Lond.* **307**, 17–22.
Arth, J. G. 1976 *J. Res. U.S. geol. Surv.* **4**, 41–48.
Auden, J. B. 1935 *Rec. geol. Surv. India* **69**, 123–167.
Auden, J. B. 1938 In *The Shaksgam Expedition, 1938* (ed. E. Shipton) Geographical Journal vol. 91, pp. 335–336.
Bard, J. P. 1983 *Earth planet. Sci. Lett.* **65**, 133–144.

Bard, J. P., Maluski, H., Matte, P. & Proust, F. 1980 *Geol. Bull. Peshawar Univ.* (*Spec. Issue*) **13**, 87–94.
Bertrand, J. M. & Debon, F. 1986 *C. r. Acad. Sci., Paris* **303**, 1611–1614.
Brookfield, M. E. 1980 *AEEi Acad. Naz. Lincei Memorie* **59**, 248–253.
Brookfield, M. E. 1981 In *Metamorphic tectonites of the Himalaya* (ed. P. S. Saklani), pp. 1–14. New Delhi: Today and Tomorrow Publishers.
Brookfield, M. E. & Reynolds, P. H. 1981 *Earth planet. Sci. Lett.* **55**, 157–162.
Broughton, R. D. Windley, B. F. & Jan, M. Q. 1985 *Geol. Bull. Peshawar Univ.* **18**, 119–136.
Brown, G. C., Thorpe, R. S. & Webb, P. C. 1984 *J. geol. Soc. Lond.* **141**, 411–426.
Burchfield, C. & Royden, L. 1985 *Geology* **13**, 679–682.
Burg, J.-P., Guiraud, M., Chen, G. M. & Li, G. C. 1984*a* *Earth planet. Sci. Lett.* **69**, 391–400.
Burg, J.-P., Brunel, M., Gapais, D., Chen, G. M. & Liu, G. H. 1984*b* *J. struct. Geol.* **6**, 535–542.
Clemens, J. D. & Vielzeuf, D. 1987 *Earth planet. Sci. Lett.* **86**, 287–306.
Clemens, J. D. & Wall, V. J. 1981 *Can. Mineralogist* **19**, 111–131.
Coward, M. P. & Butler, R. H. W. 1985 *Geology* **13**, 417–420.
Coward, M. P., Jan, M. Q., Tarney, J., Thirlwall, M. & Windley, B. F. 1982 *J. geol. Soc. Lond.* **139**, 299–308.
Coward, M. P., Windley, B. F., Broughton, R., Luff, I. W., Petterson, M. G., Pudsey, C., Rex, D. & Khan, M. A. 1986 In *Collision tectonics* (eds. M. P. Coward & A. Ries), Special Publication of the Geological Society of London no. 19, pp. 203–219.
Coward, M. P., Butler, R. H. W., Asif Khan, M. & Knipe, R. J. 1987 *J. geol. Soc. Lond.* **144**, 377–391.
Debon, F., Zimmermann, J. L. & Bertrand, J. M. 1986*a* *C. r. Acad. Sci., Paris* **303**, 463–468.
Debon, F., Le Fort, P., Sheppard, S. M. F. & Sonet, J. 1986*b* *J. Petr.* **27**, 219–250.
Debon, F. Le Fort, P., Dautel, D., Sonet, J. & Zimmerman, J. L. 1987 *Lithos* **20**, 19–40.
Deniel, C., Vidal, P., Fernandez, A., Le Fort, P. & Peucat, J. 1987 *Contr. Miner. Petr.* **96**, 78–92.
Desio, A. 1964 Geological tentative map of the western Karakoram, scale 1:500,000. Institute of Geology, Milan University.
Desio, A. 1979 In *Geodynamics of Pakistan* (ed. A. Farah & K. A. De Jong), pp. 111–124. Quetta: Geological Survey of Pakistan.
Desio, A., 1980 *Geology of the Upper Shaksgam Valley, Northeast Karakoram, Xinjiang.* (196 pages.) Holland: Brill-Leiden.
Desio, A. & Mancini, E. G. 1974 *Atti Accad. naz. Lincei Memorie* **12**, 79–100.
Desio, A. & Martina, E. 1972 *Boll. Soc. geol. Ital.* **91**, 283–314.
Desio, A. & Zanettin, B. 1970 *Geology of the Baltoro Basin.* (308 pages.) Leiden: Brill.
Desio, A., Tangiorgi, E. & Ferrara, G. 1964 *Report of XXII Sess. India, Intern. Geol. Congr. Vol.* 11, pp. 479–496.
Desio, A., Martina, E., Spadea, P. & Notarpietro, A. 1985 *Atti Accad. naz. Lincei Memorie* **18**, 3–53.
England, P. C. & Searle, M. P. 1986 *Tectonics* **5**, 1–14.
England, P. C. & Thompson, A. B. 1984 *J. Petr.* **25**, 894–928.
England, P. C. & Thompson, A. B. 1986 In *Collision tectonics* (ed. M. P. Coward & A. C. Ries), special publication of the Geological Society of London no. 19, pp. 67–82.
Foley, S. F., Venturelli, G., Green, D. H. & Toscani, L. 1987 *Earth Sci. Rev.* **24**, 81–134.
Gansser, A. 1964 Geology of the Himalayas. (298 pages.) London: J. Wiley.
Hanson, G. N. 1978 *Earth planet. Sci. Lett.* **38**, 26–43.
Harris, N. B. W., Pearce, J. A. & Tindle, A. G. 1986 In *Collision tectonics* (ed. M. P. Coward & A. Ries), Special Publication of the Geological Society of London no. 19, pp. 67–82.
Harte, B. & Dempster, T. J. 1987 *Phil. Trans. R. Soc. Lond.* A **321**, 105–127.
Henderson, P. (ed.) 1984 *Rare Earth Element Geochemistry. Developments in Geochemistry*, 2. (510 pages.) Amsterdam: Elsevier.
Herren, E. 1987 *Geology* **15**, 409–413.
Jaupart, C. & Provost, A. 1985 *Earth planet. Sci. Lett.* **73**, 385–397.
Klootwijk, C. J. 1979 In *Structural geology of the Himalaya* (ed. P. S. Saklani), pp. 307–360. New Delhi: Today and Tomorrow Publishers.
Le Fort, P. 1981 *J. geophys. Res.* **86**, 10545–10568.
Le Fort, P., Michard, A., Sonet, J. & Zimmerman, J. L. 1983 In *Granites of the Himalayas, Karakoram and Hindu Kush* (ed. F. A. Shams), pp. 377–387. Institute of Geology, Punjab University, Lahore.
Le Fort, P., Cuney, M., Deniel, C., France-Lanord, C., Sheppard, S. M. F., Upreti, B. N. & Vidal, P. 1987 *Tectonophysics* **134**, 39–57.
Lydekker, R. 1883 *Mem. geol. Surv. India* **22**, 108–122.
Molnar, P. 1984 *A. Rev. Earth planet. Sci.* **12**, 489–518.
Molnar, P. & Tapponnier, P. 1975 *Science, Wash.* **189**, 419–426.
Parrish, R. & Tirrul, R. 1988 *Geology.* (Submitted.)
Patriat, P. & Achache, J. 1984 *Nature, Lond.* **311**, 615–621.
Pearce, J. A., Harris, N. B. W. & Tindle, A. G. 1984 *J. Petr.* **25**, 956–983.
Petterson, M. G. & Windley, B. F. 1985 *Earth planet. Sci. Lett.* **74**, 45–57.
Pinet, C. & Jaupart, C. 1987 *Earth planet. Sci. Lett.* **84**, 87–99.

PHILOSOPHICAL TRANSACTIONS OF THE ROYAL SOCIETY A MATHEMATICAL, PHYSICAL & ENGINEERING SCIENCES

Powell, C. McA. & Vernon, R. H. 1979 *Tectonophysics*, **54**, 25–43.
Prior, D. J. 1987 *J. metamorph. Geol.* **5**, 27–39.
Pudsey, C. J. 1986 *Geol. Mag.* **123**, 405–423.
Pudsey, C. J., Coward, M. P., Luff, I. W., Shackleton, R. M., Windley, B. F. & Jan, M. Q. 1985 *Trans. R. Soc. Edinb.* **76**, 463–479.
Reynolds, R. H., Brookfield, M. E. & McNutt, R. H. 1983 *Geol. Rdsch.* **72**, 981–1004.
Rock, N. M. S. 1984 *Trans. R. Soc. Edinb.* **74**, 193–227.
Rutter, M. J. & Wyllie, P. J. 1988 *Nature, Lond.* **331**, 159, 160.
Schneider, H. J. 1957 *Geol. Rdsch.* **46**, 426–476.
Searle, M. P. 1986 *J. struct. Geol.* **8**, 923–936.
Searle, M. P., Windley, B. F., Coward, M. P., Cooper, D. J. W., Rex, A. J., Rex, D., Tingdong, L., Xuchang, X., Jan, M. Q., Thakur, V. C. & Kumar, S. 1987 *Bull. geol. Soc. Am.* **98**, 678–701.
Searle, M. P., Rex, A. J., Tirrul, R., Rex, D. C. & Barnicoat, A. 1988 *Bull. geol. Soc. Am.* (In the press.)
Shvolman, V. A. 1978 *Himalayan Geol.* **8**, 369–378.
Tahirkheli, R. A. K., Mattauer, M., Proust, F. & Tapponier, P. 1979 In *Geodynamics of Pakistan* (ed. A. Farah & K. A. De Jong,) pp. 125–130. Quetta: Geol. Surv. Pakistan.
Tapponnier, P., Mattauer, M., Proust, F. & Carsaigneau, C. 1981 *Earth planet. Sci. Lett.* **52**, 355–371.
Thakur, V. C. & Misra, D. K. 1984 *Tectonophysics* **101**, 207–220.
Thompson, R. N., Morrison, M. A., Hendry, G. L. & Parry, S. J. 1984 *Phil. Trans. R. Soc. Lond.* A **310**, 549–590.
Vidal, P., Cocherie, A. & Le Fort, P. 1982 *Geochim. cosmochim. Acta* **64**, 2274–2292.
Wickham, S. M. 1987 *J. geol. Soc. Lond.* **144**, 281–297.
Zanettin, B. 1964 *Geology and petrology of the Haramosh-Mango Gusar area.* Leiden: Brill.
Zeitler, P. K. 1985 *Tectonics* **4**, 127–151.

Note added in proof (3 *March* 1988). Here we discuss the BPU in relation to petrogenetic models for other post-collisional granites, especially those in the Himalayan belt. The model of Le Fort (1981) for the generation and emplacement of the Manaslu granite is now widely applied to other post-collisional granites of the High Himalaya. It differs from that proposed here for the BPU, consistent with the outstanding differences in chemical, mineralogical and isotopic characteristics. Therefore it is important to emphasize that although the High Himalayan petrogenetic model is convincing, it should not be accepted as a general model for all melts derived by partial melting of crustal sources (see Clemens & Vielzeuf 1987).

Discussion

J.-M. Bertrand (*Centre de Recherches Pétrographiques et Géochimiques, France*). The tectonic evolution of the Karakoram presented by the Leicester group fits well with our observations on the lower Braldu Valley and along two N–S sections (Hoh Lunghma and Panmah Valleys). However, I would like to comment briefly on two points of disagreement.

(1) The discrimination between several lithological groups or formations and especially the reference to the Ganschen and Dumordo Formations first described by Desio (1964) is very doubtful as the same rock associations may be found in most of them; for example the mafic and ultramafic units exist both in the Ganschen Formation and Dumordo Formation. If several distinctive formations have to be distinguished among the Karakoram gneisses, they have to be assessed upon very detailed sections.

(2) From small-scale and large-scale structures and from the recorded metamorphic evolution, we tend to divide the M2 metamorphic event into two distinct events, our D1 and D2 (Bertrand & Debon 1986); M1 has not been recognized on the area studied. D2 corresponds to superimposed low-pressure mineral assemblages and to large-scale recumbent folding. In contrast to the clear separation between D1 and D2, outlined by emplacement of

post-D1 pre-D2 leucogranitic bodies, a continuous evolution between D2 and a dome-forming D3 event is assumed, the latter being followed shortly by the emplacement of the Baltoro granite. In our opinion, the D2–D3 low-pressure metamorphism, which is not restricted to the margins of the Baltoro granite, cannot be interpreted as contact metamorphism but is, more likely, a dome-related thermal anomaly, the last consequence of which being probably the emplacement of the Baltoro granite. Such an interpretation is supported by the complete similarity in tectonic and metamorphic evolution between the Dassu dome and the high-grade gneisses and migmatites occurring just south of the contact of the Baltoro granite.

Reference

Bertrand, J. M. & Debon, F. 1986 *C. r. Acad. Sci., Paris* (II) **17**, 1611–1614.

A. J. Rex and M. P. Searle. We agree with Dr Bertrand that there is insufficient detail to distinguish the Ganschen and Dumordo Formations in any stratigraphic sense, hence their omission from our maps and their loose definition as units. The mafic–ultramafic blocks are exotic to both units, with which they are in tectonic contact.

The M1 metamorphic event is only regionally present around the Hushe and Thalle Valleys, east of the area studied by Bertrand & Debon (1986). We have documented an increase in temperature of *ca.* 75 K from Bardumal to Paiju approaching the contact of the BPU along the Baltoro glacier (Searle *et al.* 1988), which we have modelled here as the thermal upwarping of pre-36 Ma M2 isograds around the 21 Ma M3 aureole isotherms of the BPU. This temperature increase is restricted to the margin of the BPU and although it may be consequential and hence part of regional M2, we suggest that it is a thermal overprint after initial uplift of the M2 isograds. The 'dome-shaped thermal anomalies' around the Dassu and Panmah domes are, in our opinion, formed by post-metamorphic folding of isograds due to thrust culmination.

PHILOSOPHICAL TRANSACTIONS OF THE ROYAL SOCIETY A MATHEMATICAL, PHYSICAL & ENGINEERING SCIENCES